Synthesis, Molecular Modeling and Biological Evaluation of Novel Imatinib Derivatives as Anticancer Agents

Fulya Günay
Yildiz Technical University: Yildiz Teknik Universitesi
Sevcan Balta
Yildiz Teknik Universitesi
Yuk Yin Ng
Istanbul Bilgi University: Istanbul Bilgi Universitesi
Özlem Ulucan
Istanbul Bilgi University: Istanbul Bilgi Universitesi
Zuhal Turgut
Yildiz Technical University: Yildiz Teknik Universitesi
Omer Tahir Gunkara (omerrrgunkara@hotmail.com)
Yildiz Teknik Üniversitesi https://orcid.org/0000-0003-3528-5045

Research Article

Keywords: imatinib derivatives, tyrosine kinase inhibitors, MTT, BCR-ABL inhibitors, leukemia, molecular docking

Posted Date: April 15th, 2021

DOI: https://doi.org/10.21203/rs.3.rs-392724/v1

Abstract

Different derivatives of imatinib, the first targeted BCR-ABL fusion tyrosine kinase inhibitor, were synthesized by a 3-step reaction method. Firstly, benzamide derivative was obtained then aryl piperazine groups or morpholine were linked by the S_N2 reaction. Lastly, palladium catalyzed C-N coupling reaction was conducted with hetaryl amine groups. The structures of the new compounds were characterized by spectroscopic methods. For quantitative evaluation of the biological activity of the compounds, MTT assays were performed, where four BCR-ABL negative leukemic cell lines (Jurkat, REH, NALM6 and MOLT4), one BCR-ABL+ cell line (K562) and one non-leukemic cell line (Hek293T) were incubated with various concentrations of the derivatives. Although imatinib was specifically designed for the BCR-ABL protein, our results showed that it was also effective on BCR-ABL negative cell lines except for REH cell line. Molecular docking simulations suggest that except for compound 6, the compounds prefer a DFG-out conformation of the ABL kinase domain. Among them, compound 10 has the highest affinity for ABL kinase domain that is close to the affinity of imatinib. The common rings between compound 10 and imatinib adopt exactly the same conformation and same type of interactions in the ATP binding site with the ABL kinase domain.

Introduction

Imatinib mesylate (Fig1) is the first generation of FDA approved protein-tyrosine kinase inhibitor (Gleevec®, STI-571), especially specific to target c-ABL (the Abelson proto-oncogene) and BCR-ABL (the Breakpoint cluster region) gene products. It has a potent inhibitor to treat wild-type (WT) KIT proto-oncogene (receptor tyrosine kinase) and certain mutant KIT isoforms. [1] Also, there are studies described about its usage as potent PDGFR inhibitor [2]. With the discovery of imatinib mesylate, it has almost revolutionized the treatment of chronic myelogenous leukemia (CML). And it has become the standard of care for treating patients with metastatic gastrointestinal stromal tumors [1].

Imatinib contains 2-(phenylamino)pyrimidine heterocycle core that functions for targeting BCR-ABL activity leading to decrease tyrosine kinase activity; methyl group on this core occupies the selectivity to BCR-ABL; aryl piperazine core increases oral bioavailability and pyrimidine core occupies cellular activity [3].

There are three different general methods for the synthesis of imatinib mesylate [4-9].There are also some patents[10-15] which imatinib is obtained by directly reacting the commercially sold aminopyrimidine and the aryl piperazine derivatives. Moreover, there are flow-based [16-18], polymer-supported [20], copper-catalyzed [21], palladium catalyzed [22], BrettPhos-catalyzed [23-24] methods for synthesizing imatinib.

In treatment of CML, FDA-approved tyrosine kinase inhibitors such as imatinib are commonly used. Tyrosine specific protein kinases are effective in regulating a wide range of cellular activities such as growth, development, differentiation, protection of vitality, proliferation, apoptosis, adhesion to surface, emigration, deformation of cells. It is well known that deregulation of these cellular processes is due to

hyper-activation of tyrosine kinase activity in cancer cells compared to normal cells [25]. Tyrosine kinases use ATP as a phosphate group source for phosphorylation. The main mechanism of action of tyrosine kinase inhibitors is to prevent displacement of one phosphate group on adenosine triphosphate (ATP) to the specific tyrosine amino acid in the substrate protein and thereby reducing the activation of signal flow pathways. In other words, tyrosine kinase inhibitors are in competition with ATP [26-28].

Imatinib is specific for the tyrosine kinase domain in ABL and it has been reported that treatment with BCR-ABL inhibitors, significantly reduces the application of hematopoietic cell transplantation for treatment of CML [29]. It binds ABL1 kinase in ATP binding site and stabilizes an inactive conformation of the catalytic domain where the well-known “DFG” triad is in an out conformation [1].

After prolonged treatment of imatinib, due to mutations at kinase domain site in ATP binding site the drug activity changes. Over-stimulated BCR-ABL1 fusion protein causes genomic instability in CML stem cells and causes more than 50 hotspot mutations to accumulate in the ABL1 kinase domain. Complexity or having more than one mutation also changes the patient's outcome against the drug. ABL1 point mutations reduce the accessibility of the drug's binding site, limiting the enzyme's flexibility [29-30].

For this reason, PD180970, CGP76030, BMS-354825, AMN 107 or Nilotinib and more recently AP24534 have been developed. There are also novel approaches (Farnesyltransferase inhibitors; such as SCH66336 and the Proteasome inhibitor Bortezomib) to imatinib resistance that have been reported to have growth inhibitory properties on leukemia [31-37].

In this study, it was aimed to synthesize and investigate the biological activity of new imatinib derivatives that potently inhibit the growth of cancer cells. The designed compounds were synthesized, and their structural formula were confirmed by different spectral data. Anti-cancer activities of all the newly synthesized compounds were examined by MTT ((3-(4,5-dimethylthiazol-2-yl)-2,5-diphenyltetrazolium bromide) assay.

Additionally, we performed extensive molecular docking simulations to evaluate the binding preference of newly synthesized compounds to different conformations of wild type ABL and BRAF kinases. Except for compound 6, the newly synthesized imatinib analogs prefer a DGF-out conformation of ABL kinase. Among all newly synthesized analogs, compound 10 has the highest affinity for ABL kinase domain which is comparable to the affinity of imatinib for the ABL kinase domain. Analysis of molecular interactions revealed similarities between binding patterns of compound 10 and imatinib. Despite predicted to be a potential target, the new imatinib analogs have lower affinities for BRAF kinase compared to ABL kinase.

Results And Discussion

Chemistry

The general procedure for the synthesis of novel imatinib derivatives is outlined in Scheme 1. In the first step, *N*-(3-bromo-4-methylphenyl)-4-(chloromethyl)benzamide (**3**) was obtained using 4-(chloromethyl)benzoyl chloride (**1**) and 3-bromo-4-methylaniline (**2**) in inert atmosphere [16-17].

In the second step, bromobenzamide derivatives (**4a-c**) were obtained by performing a substitution reaction (S_N2) using different cyclic secondary amine compounds.

As an cyclic secondary amine group; 2-(1-piperazinyl)pyrimidine was used for preparation of compound **4a. (**Because pyrimidine and its derivatives are found in nucleobases which composed DNA and RNA and they have broad spectrum of biological effects including anticancer activities [38], it was used as an aryl piperasine group in compound **5** and **7**.) And 1-(2,3,4-trimethoxybenzyl)piperazine dihydrochloride (called also as Trimetazidine dihydrochloride) was used for preparation of compound **4b** as an aryl piperazine group, in compounds **6** and **10**. (It was selected due to its immunomodulating [39] and antineoplastic [40] properties.)

For preparation of **4a** and **4b**, compound **3** and aryl piperazine groups were dissolved in dry acetone under inert atmosphere. Then, overheated K_2CO_3 was added to the reaction mixture. The mixture was heated and stirred overnight under inert atmosphere. Aryl piperazine derivatives show specific inhibition activities in cancer cells [41-44].

Morpholine moiety also plays critical role in several inhibition activities and used as anticancer agents [45-47], because of that reason, we preferred to use as aryl piperazine group for preparation of compound **4c**. In this reaction; compound **3** was taken into a round bottom flask and morpholine was added onto it. The reaction mixture was sonicated without solvent.

In the final step, novel imatinib derivatives (**5-10**) were synthesized by a Buchwald Hardwing coupling reaction between hetaryl primary amines and aryl bromide (**4a-c**). (Dibenzylidenacetone) dipalladium(0) was used as a catalyst and Xphos was used as a ligand in these reactions. Potassium *tert*-butoxide was also added to the reaction mixtures as a base. Several aromatic amine [2-amino-4-methylpyrimidine, 2-amino-pyrazine, or 2-amino-4-methylpyridine] were used.

All of the crude products were purified with flash chromatography.

Characteristics of Newly Synthesized Compound According to Lipinski's Rule of Five

Because oral using of pharmaceutical compounds is easier, the new molecules were evaluated by Lipinski Rule of 5, using Medchem Designer program and https://www.molinspiration.com [48], comparing with imatinib, (Table-S2)

In vitro anti-proliferative activity

To evaluate the pharmaceutical potential, the newly synthesized imatinib derivatives 5-10 were tested for their in vitro anticancer activity in the BCR-ABL positive leukemic cell line K562, BCR-ABL negative

leukemic cell lines, Nalm-6, Molt-4, REH and Jurkat, and non-leukemic human embryonic kidney tissue Hek293T cell line by using the MTT assay. As control imatinib mesylate was used as the reference compound. The corresponding results were expressed as IC_{50} values and presented in Table 1 and Fig3. All cells were incubated with various concentrations of the derivatives for 24 hours and the growth inhibition rate was measured between (0.3-200μM) was presented in Fig2 and Table S3.

In K562 cells, we observed the highest growth inhibition with imatinib mesylate. After 24 hours, more than 70% (70.3%) cells with killed after the incubation. From the newly synthesized derivatives, only compound 10 (63.11%), and in less extent compound 9 (55.03%), were also able to achieve high growth inhibition in the K562 cell line. Moreover, the IC_{50} value of compound 10 (35.04 μM) is lower compared to imatinib mesylate (78.37 μM) indicating K562 cell line is more sensitive to the newly synthesized derivative than the reference compound. The other derivatives showed significant lower growth inhibition compared to imatinib mesylate.

In BCR-ABL negative cell lines, growth inhibition by the compounds was also observed. In consistent with K562 cells, compound 6, 9 and 10 exhibited anti-proliferative activities in nearly all BCR-ABL negative cell lines. In Nalm-6 and Jurkat cell lines, we observed over 50% inhibition of cell growth. The maximum inhibitory activity of compound-6 and compound-9 on Nalm-6 cells were both 59.14% and 60.82%. The IC_{50} values were 47.96 μM and 1.639 μM respectively. Compound-10 showed 72.04% with IC_{50} of 28.73 μM in Nalm6 cells. The effects of imatinib and its derivatives on Jurkat cells were similar to the results obtained with Nalm-6 cells. Again, the best growth inhibition was obtained with imatinib (72.79%). In Molt4 cell lines, all compounds showed moderate or low growth inhibition effect. Interestingly, only compound-10, showed over 50% inhibition on Molt-4 cells. REH cells appear to be less sensitive to the newly synthesized derivatives. Up to about 40% inhibition was seen in REH cells, including imatinib (see FigS44).

In general, according to MTT assay results, the compounds with 2,3,4-trimethoxybenzyl in aryl piperazine group (R^1, Table-1), (compound 6 and 10) exhibited high anticancer activity on all cell lines, except REH. Whereas instead of aryl piperazine ring, morpholine substituted analogs (compound 8 and 9) displayed somewhat relatively lower activity, and the analogs with pyrimidine ring in aryl piperazine group (compound 5 and 7) were characterized by very poor activity.

Also, the results show that there was not so much difference between 2-aminopyrimidine and 2-aminopyrazine heterocyclic ring system (R^2, Table-1), (compound 5-7).

High growth inhibitory activity was also obtained for pyrimidine-substituted derivatives. And also, the pyridine linked analogs (compound **9-10**) exhibited high anticancer activity than pyrimidine and pyrazine group.

When we examine the results of 24-hour cell culture studies, inhibition of the compounds can be listed as imatinib>10 > 9 > 6 > 7> 8 > 5 in descending order.

ABL1 Expression analysis

Although imatinib was specifically designed as a drug for the BCR-ABL fusion gene product, our results showed that it was also effective in BCR-ABL negative cell lines. One explanation can be given that all the compounds, including imatinib mesylate, are targeted to the kinase domain of ABL protein. The ABL protein, encoded by the ABL1-gene, is a non-receptor tyrosine kinase which is constitutively expressed in all cells. ABL protein is activated in response to several stimuli such as cell adhesion, cytokines, growth factors, DNA damage and other signals. Activation of ABL protein will resulted in migration, cell proliferation, differentiation and apoptosis. Although the BCR-ABL negative cell line do not expressed the fusion protein, but they all expressed the endogenous ABL protein, which can be targeted also by the compounds. To support this, we have compared the gene expression of ABL1 in the cell lines by microarray data available in the literature. Indeed, we observed that ABL1 gene is highly expressed in these cell lines, with the highest in K562 cell line.

Secondly, other tyrosine kinase proteins with similar kinase domain as the ABL1 protein can also be targeted by the compounds as it is predicted with the SEA search tool.

Fig4 depicts the expression level of the gene ABL1 in the cell lines. The mean expression level for ABL1 varies between 8.3 (Jurkat) and 9.1 (K562). Even though the one-way ANOVA results suggest significant difference (P-value < 0.01), the log2 fold change values (< 0.8) we obtained from binary comparisons support no difference in ABL1 expression level among the cell lines.

The comparable expression level of ABL1 in the studied cell lines may explain why the compounds 6, 9 and 10 show no cell line specific inhibitory effect.

Molecular docking

Protein targets for novel imatinib analogs

Similarity Ensemble Approach (SEA) [49] search tool predicted several proteins as target for the novel imatinib analogs (see Table S4). We picked three most appropriate targets that are common to lists of imatinib and its newly synthesized analogs and decided further to assess them using molecular docking simulations. Among our 3 putative targets, which are Atypical chemokine receptor 3 (P25106), Serine/threonine-protein kinase BRAF (Uniprot ID: P155056) and BCR/ABL p210 fusion protein (A1Z199), Atypical chemokine receptor 3 does not have a crystal structure, hence, we could not perform molecular docking simulations for this protein.

BCR/ABL fusion protein has a constitutively activated ABL tyrosine kinase domain. Imatinib inhibits the catalytic activity of BCR/ABL by binding to an inactive conformation of the ABL kinase domain [50]. Since our newly synthesized compounds are analogs of imatinib, it is not surprising that ABL kinase is one of the putative targets for our compounds. Superposition of various structures reported, and molecular dynamic simulation studies performed show a great conformational flexibility in ABL protein kinase [50-52]. This conformational plasticity is the reason for the differences in inhibitor binding site,

which has been exploited for inhibitor selectivity and affinity optimization. The conformation of the DFG motif has long been known for its effect on the binding pocket. Four main conformations have been reported for the highly conserved DFG motif. Those conformations can be listed as the active conformation, the DFG-out conformation, the DFG-flip conformation and the Src-like inactive conformation. We evaluated all crystal structures of wild-type human ABL kinase domain in the Protein Databank [53-54] and selected 8 of them for molecular docking analysis (see supplementary Table S6). These selected structures represent inactive DFG-out conformation (2HYY [52], 2E2B [54], 2HZ0 [52], 3CS9 [56] and 3UE4 [57]), Src-like inactive conformation (4CY8 [58]), intermediate DFG-flip conformation (2HZI [52]) and active conformation (2HZ4 [52]).

Table 2 summarizes the results of the docking simulations of imatinib and its 6 newly synthesized analogs to the 8 different conformations of wild-type human ABL kinase domain. We assessed the reliability of docking results using the percentage of independent runs that converge to the same binding conformation. We assumed a docking simulation result reliable when at least 20 % of the independent runs resulted in this particular binding conformation (see Table S6).

This assumption is based on the re-docking calculations that we performed where we docked the original ligands to the protein conformations found in the crystal structures. The sizes of the clusters that we obtained from the re-docking calculations vary between 20 and 100 conformations (see Table S6 and Table S8). Our results presented in Table 1 suggest that imatinib binds to different conformations of ABL however with varying free energies of binding (9.6 – 14.7 kcal/mol). According to the free energies given in the table, imatinib prefers DFG-out conformations of the ABL kinase domain, which is also well reported in the literature [50]. The analog compounds 5, 7, 8, 9 and 10 have a similar tendency with imatinib. However, compound 6 seems to prefer the intermediate conformation where the DFG motif adopts a flipped conformation (see Table 3). Among all the newly synthesized analogs compound 10 has the most favorable free energy of binding (-14.2 kcal/mol) that is closest to the free energy of binding for imatinib (-14.7 kcal/mol). Evaluating molecular docking and MTT assay results together we decided to compare the interactions of imatinib and compound 10 with ABL kinase domain in details. As provided in Fig5, two molecules adopt overall a similar binding mode despite some local differences. The common rings (the methylbenzene, the benzamide and the N-methylpiperazine rings) between two molecules adopt exactly the same conformation and contribute to the same type of interactions. The overlapping in binding modes is also true for Compound 5, 7 and 8 (see FigS45, S47 and S48) and partially true for Compound 9 (see FigS49). However, compared to imatinib, compound 6 adopts a very distinct binding mode (see FigS46).

Similar to ABL kinase, for BRAF kinase different conformational states reported in literature as well; inactive DFG-out conformation (1UWH59, 4KSP60 and 4JVG61), Src-like inactive conformation (3C4C62 and 5CSW63) and active conformation (2FB864 and 3D4Q65). The results of molecular docking to wild type human BRAF kinase domain is tabulated in Table 3. As seen in the table, the new imatinib analogs have lower affinities for BRAF kinase compared to ABL kinase.

Conclusion

The anti-proliferative activities in vitro showed that compound 10 gives results close to imatinib. Although imatinib was specifically designed as a drug for the BCR-ABL fusion gene, our results showed that, it was also effective for Jurkat and Nalm-6 cells, which are BCR-ABL negative cells. We also found that Compound 6 and 9 were relatively effective in Nalm-6 and Jurkat cells.

To sum up, this study introduces a novel successful design for imatinib derivatives as the potential antitumor agents. These compounds possess a simple molecular structure and are easy to synthesize which makes them very attractive for further exploration as kinase inhibitors with application in cancer therapy.

Materials And Methods

Chemistry

General

All chemicals used were purchased from Merck and Aldrich without further purification. Trimetazidine HCl was obtained from World Medicine Drug Company (Fisher Scientific, CAS Number: 13171-25-0), Imatinib was purchased from Sigma (SML1027-100MG). Sonication was performed in an Intersonik ultrasound cleaner (model: MIN4) with a frequency of 25 kHz, an US output power of 100 W, a heating 200 W. Heidolph RV Laborata 4000 rotary evaporator was used evaporation the solvent. A TLC Merck 5554 with silica gel layers with fluorescent indicator and a Camag (254/366 nm) UV lamp were used. The melting points of the pure materials were measured on Stuart apparatus. Fourier Transform Infrared (FTIR) spectra of the starting materials and the obtained products were taken on a “Perkin Elmer Spectrum One” FTIR spectrometer by ATR technique. Nuclear magnetic resonance (^{1}H and ^{13}C NMR) spectra were obtained from a “Bruker 500 MHz” spectrometer in CDCl3. Chemical shifts were reported in parts per million (ppm) with respect to internal standard TMS. LC-MS spectra were obtained by Agilient 6200 series TOF/6500 series TOF/Q-TOF Mass Spectrometer. All crude products were purified with Teledyne Isco CombiFlash Rf 200 system and RediSep Rf Gold Silica Columns.

General procedure for the synthesis of intermediate containing benzamide

1 mmol (186.05 mg) 3-bromo-4-methylaniline (2) (see Scheme 1) was placed in a two neck round bottom flask. It was dissolved in dry DCM (4 mL) under inert atmosphere at 0°C. 1 mmol (138.205 mg) of overheated K_2CO_3 was added the reaction mixture and stirred at same temperature. After that, 1 mmol (189.04 mg) 4-chloromethylbenzoylchloride was dissolved with dry DCM (4 mL) and injected dropwise into the reaction medium. While continuing the addition, yellow crystals formed in the reaction medium. The mixture was stirred at 0°C for 1 hour. After completion of the reaction, the yellow crystals were filtered, washed with DCM and dried [16-18].

***N*-(3-Bromo-4-methylphenyl)-4-(chloromethyl)benzamide (3):** Yellow solid, (This compound was crystallized with DCM, yield: 98%, Rf: 0.54 (1:3 Ethylacetate/n-Hexane), m.p. 157°C); IR (ATR) n_{max} 3452 (NH), 3284, 2985, 1641 (C=O), 1577, 1499, 1441, 1384, 1299 cm^{-1}; ^1H NMR [18] (600 MHz, $CDCl_3$): δ = 2.38 (s, 3H, CH_3), 4.63 (s, 2H, CH_2), 7.21 (d, J=8.2 Hz, 1H, Ar-H) , 7.47 (d, J=1.5 Hz, 1H, Ar-H), 7.51 (d, J=8.5 Hz, 2H, Ar-H), 7.84 (brds, 1H, NH), 7.85 (dd, J= 8.5,1.7 Hz, 2H, Ar-H) 7.89 (s, 1H, Ar-H) ppm; ^{13}C NMR [18] (150 MHz, $CDCl_3$): δ = 22.35 (CH_3), 45.29 (CH_2), 119.17 (CAr), 123.95 (CAr), 124.89 (CAr), 127.49 (CAr), 128.99 (2xCAr), 130.91 (2xCAr), 134.21 (CAr), 134.59 (Cq), 136.55 (Cq), 141.42 (Cq), 164.97 (C=O) ppm.

General procedure for the synthesis of intermediates containing aryl piperazine

0.3 mmol (101.59 mg) *N*-(3-Bromo-4-methylphenyl)-4-(chloromethyl)benzamide (3) and 0.39 mmol aryl piperazine [2-(piperazin-1-yl)pyrimidine or 1-(2,3,4-trimethoxybenzyl) piperazine dihydrochloride)] were taken into a round bottom flask. The starting materials were dissolved in dry acetone (10 mL) under inert atmosphere. Then, 0.9 mmol (124.38 mg) of overheated K_2CO_3 was added to the reaction mixture. The mixture was heated and stirred at 55 °C overnight under inert atmosphere. After completion of the reaction, the reaction mixture was filtered and the solvent was evaporated under reduced pressure. The crude products 4a and 4b were purified using flash chromatography.

N-(3-Bromo-4-methylphenyl)-4-((4-(pyrimidin-2-yl)piperazin-1-yl)methyl)benzamide (4a): Brownish gummy solid (This compound was purified by flash column chromatography using ethylacetate/*n*-hexane 5:1 as eluent, Rf:: 0.45 (5:1 ethylacetate/*n*-hexane), yield : 60%, m.p. 105°C); IR (ATR) n_{max} 3283 (br) (NH), 3081 (w), 2991 (w), 2947 (w), 1737 (s) (C=O) 1252 (vs), 1017 (vs) cm^{-1}; ^1H NMR (500 MHz, $CDCl_3$): δ 2.37 (s, 3H, CH_3), 2.50 (t, J= 2.4 Hz, 4H, N-CH_2), 3.60 (s, 2H, CH_2), 3.83 (t, J= 2.4 Hz, 4H, N-CH_2), 6.48 (t, J= 4.7 Hz, 1H, Ar-H), 7.19 (d, J= 8.3 Hz, 1H, Ar-H), 7.46 (d, J= 8.4 Hz, 2H, Ar-H), 7.48-7.49 (m, 1H, Ar-H), 7.81 (d, J= 8.2 Hz, 2H, Ar-H), 7.88 (d, J= 2.2 Hz, 1H, Ar-H), 7.94 (brds, 1H, NH), 8.29 (d, J= 4.7 Hz, 2H, Ar-H) ppm; ^{13}C NMR (125 MHz, $CDCl_3$) δ 22.3 (CH_3), 43.7 (2x*N*-CH_2), 53.0 (2x*N*-CH_2), 62.6 (CH_2), 109.8 (CAr), 119.2 (CAr), 123.9 (CAr), 124.8 (Cq), 127.1 (2xCAr), 129.4 (2xCAr), 130.8 (CAr), 133.5 (Cq), 133.9 (Cq), 136.8 (Cq), 142.6 (Cq), 157.7 (2xCAr), 165.5 (C=O) ppm; HRMS (ESI^+) m/z calcd for $[C_{23}H_{24}BrN_5O]+H^+$ 468.1222, found 468.1215 $([C_{23}H_{24}BrN_5O_4]+H)^+$.

***N*-(3-Bromo-4-metylphenyl)-4-((4-(2,3,4-trimethoxybenzyl)piperazin-1-yl)methyl)benzamide (4b):** Pale yellowish gummy solid (This compound was purified by flash column chromatography using DCM/MeOH 10:1 as eluent, Rf : 0.54 (10:1 DCM/MeOH), yield 46.3%; m.p.135°C); IR (ATR): n_{max} 3290 (br) (NH), 2936 (m), 2819 (m), 1651 (s) (C=O), 1235 (m), 1093 (vs) cm^{-1}; ^1H NMR (500 MHz, $CDCl_3$): δ = 2.37 (s, 3H, CH_3), 2.48 (brds, 8H, N-CH_2), 3.50 (s, 2H, CH_2), 3.55 (s, 2H, CH_2), 3.85 (s, 3H, O-CH_3), 3.86 (s, 3H, O-CH_3), 3.88 (s, 3H, O-CH_3), 5.30, 6.62 (d, J = 8.20, 1.5 Hz, 1H, Ar-H), 6.64 (d, J= 8.60,1H, Ar-H) 6.98 (d, J= 8.60 Hz, 1H, Ar-H), 7.19-7.21 (dd, J=8.2, 0.5 Hz, 1H, Ar-H) , 7.27 7.40-7.42 (dd, J=1.5 0.5Hz, 1H) 7.48-7.50 (ddd, J=8.5 1.4, 0.5 Hz, 2H, Ar-H), 7.78-7.88 (ddd, J= 8.5,1.7, 0.5 Hz, 2H, Ar-H) ppm; ^{13}C NMR (125 MHz, $CDCl_3$): δ = 22.29 (CH_3), 52.84 (CH_2), 53.20 (CH_2), 55.95 (2xCH_2) 56.00 (2xCH_2), 60.68 (O-CH_3), 61.13 (O-

CH_3), 62.51 (O-CH_3), 106.96 (CAr), 119.10 (CAr), 123.86 (CAr), 124.78 (CAr), 125.16 (CAr), 126.94 (2xCAr), 129.36 (2xCAr)), 130.81 (CAr), 133.32 (Cq), 133.87 (Cq), 136.79 (Cq), 142.89 (Cq), 152.63 (Cq),152.90(Cq), 165.46 (C=O) ppm; HRMS (ESI^+) m/z calcd for $[C_{29}H_{34}BrN_3O_4]+H^+$ 569.5099, found 569.5200 $([C_{29}H_{34}BrN_3O_4]+H)^+$.

General procedure for the synthesis of intermediates containing morpholine

0.3 mmol (116.79 mg) of N-(3-Bromo-4-methylphenyl)-4-(chloromethyl)benzamide (3) was taken into a round bottom flask and 2.6 mmol (226.46 mg) morpholine was added onto it. The reaction mixture was sonicated at 55°C for 30 minutes without solvent. After completion of the reaction, the crude product (4c) was recrystallized with ethyl acetate.

N-(3-Bromo-4-methylphenyl)-4-(morpholinomethyl)benzamide (4c): Cream-white, gummy solid; (This compound was purified by crystallization with EtOAc, Rf: 0.7 (7:1 DCM/MeOH), yield 76.7%; m.p.116°C); IR (ATR) n_{max} 3268 (s) (NH), 3023 (w), 2920 (m), 1636 (vs) (C=O), 1260 (w), 1036 (vs) cm^{-1}; ^1H NMR (500 MHz, $CDCl_3$): δ = 2.38 (s, 3H, CH_3), 2.52 (brds, 4H, N-CH_2), 3.62 (s, 2H, CH_2), 3.75 (t, J= 2.5 Hz, 4H, O-CH_2), 7.20 (d, J= 8.4 Hz, 1H, Ar-H), 7.48 (m, 3H, Ar-H), 7.82 (d, J= 8.2 Hz, 2H, Ar-H), 7.92 (d, J= 2.1 Hz, 1H, Ar-H), 7.97 (brds, 1H, NH) ppm; ^{13}C NMR (125 MHz, $CDCl_3$): δ = 22.3 (CH_3), 43.3 (CH_2), 53.5 (CH_2), 62.7 (CH_2), 63.8 (CH_2), 66.6 (CH_2), 119.2 (CAr), 123.9 (CAr), 124.8 (Cq), 127.2 (2xCAr), 129.7 (2xCAr), 130.8 (CAr), 133.8 (Cq), 134.0 (Cq), 136.7 (Cq), 165.4 (C=O) ppm; HRMS (ESI^+) m/z calcd for $[C_{19}H_{21}BrN_2O_2]+H^+$ 390.2942, found 390.1805 $[(C_{19}H_{21}BrN_2O_2)+H]^+$.

General Procedure for the Synthesis of Imatinib Derivatives (5-10)

In a 10 mL oven dried schlenk tube, equipped with a rubber septum, 0.214 mmol compound 4a, 4b or 4c, 0.214 mmol corresponding aromatic amine [2-amino-4-methylpyrimidine, 2-aminopyrazine or 2-amino-4-methylpyridine] 0.297 mmol (33.4 mg) Potassium tert-butoxide, 0.01712 mmol (9.9 mg) Xphos, 0.00856 mmol (7.8 mg) Tris (dibenzylidenacetone) dipalladium(0) were added. Subsequently, 1 mL dry toluene and 1 mL dry tert-butanol were added into the tube and resulting mixture was heated and stirred at 160°C for 24 h under inert atmosphere. The reaction completion was monitored by TLC. Upon completion of the reaction, the mixture was filtered through celite, washed with DCM, then the solvent was evaporated under reduced pressure. The residue was purified by flash chromatography.

***N*-(4-Methyl-3-((4-methylpyrimidin-2-yl)amino)phenyl)-4-((4-(pyrimidin-2-yl)piperazin-1-yl)methyl)benzamide (5):** Brownish gummy solid; (This compound was purified by flash column chromatography using DCM/MeOH 10:1 as eluent, 0.54 (10:1 DCM/MeOH), yield 40%; m.p.89°C); IR (ATR) n_{max} 3280 (br) (NH), 3026 (w), 2850 (w), 1651 (s) (C=O), 1219 (w), 1029 (s) cm^{-1}; ^1H NMR (500 MHz, $CDCl_3$): δ = 2.32 (s, 3H, CH_3), 2.43 (s, 3H, CH_3), 2.52 (brds, 4H, *N*-CH_2), 3.49 (brds, 1H, NH), 3.61 (s, 2H, CH_2), 3.84 (t, J= 2.5 Hz, 4H, N-CH_2), 6.48 (t, J= Hz, 1H, Ar-H), 6.75 (brds, 1H, NH), 7.16-7.21 (m, 1H, Ar-H), 7.44-7.51 (m, 3H, Ar-H), 7.79-7.88 (m, 3H, Ar-H), 8.28-8.30 (m, 3H, Ar-H), 8.38-8.40 (m, 1H, Ar-H) ppm;

^{13}C NMR (125 MHz, $CDCl_3$): δ = 19.4 (CH_3), 22.3 (CH_3), 43.6 (2xN-CH_2), 52.9 (2xN-CH_2), 62.6 (CH_2), 109.8 (CAr), 119.1 (CAr), 123.8 (CAr), 124.7 (Cq), 127.0 (3xCAr), 129.3 (3xCAr), 130.7 (CAr), 133.3 (2xCq), 133.8 (Cq), 136.7 (2xCq), 142.5 (Cq), 157.6 (2xCAr), 161.6 (Cq), 165.5 (C=O) ppm; HRMS (ESI$^+$) m/z calcd for $[C_{28}H_{30}N_8O]+H^+$ 495.2621, found 495.2607 $[(C_{28}H_{30}N_8O)+H]^+$

***N*-(4-Methyl-3-((4-methylpyrimidin-2-yl)amino)phenyl)-4-((4-(2,3,4-trimethoxyphenyl)piperazin-1-yl)methyl)benzamide (6):** Yellowish gummy solid (This compound was purified by flash column chromatography using DCM/MeOH 7:1 as eluent, 0.50 (7:1 DCM/MeOH), yield 58.1%; dcm.p.320°C); IR (ATR) n_{max} 3293 (br) (NH), 2932 (s), 1651 (s) (C=O), 1200 (m), 1093 (vs) cm^{-1} ; ^{1}H NMR (500 MHz, $CDCl_3$): δ = 2.28 (s, 3H, CH_3), 2.41 (s, 3H, CH_3), 2.50 (brds, 8H, N-CH_2), 3.52 (s, 2H, CH_2), 3.54 (s, 2H, CH_2), 3.85 (s, 3H, O-CH_3), 3.86 (s, 3H, O-CH_3), 3.88 (s, 3H, O-CH_3), 6.59 (d, J= 5.0 Hz, 1H, Ar-H), 6.62 (d, J= 8.5 Hz, 1H, Ar-H), 6.92 (brds, 1H, NH), 6.99 (d, J= 8.5 Hz, 1H, Ar-H), 7.16 (d, J= 8.3 Hz, 1H, Ar-H), 7.38 (d, J=8.1 Hz, 1H, Ar-H), 7.44 (d, J= 7.3 Hz, 1H, Ar-H), 7.78 (d, J= 8.1 Hz, 2H, Ar-H), 8.03 (brds, 1H, NH), 8.25 (d, J= 5.0 Hz, 1H, Ar-H), 8.33 (d, J= 1.9 Hz, 1H, Ar-H) ppm; ^{13}C NMR (125 MHz, $CDCl_3$): δ = 17.6 (CH_3), 24.2 (CH_3), 52.7 (2xN-CH_2), 55.9 (2xN-CH_2), 61.2 (CH_2), 106.1 (CAr), 112.3 (CAr), 115.2 (CAr), 123.9 (Cq), 127.0 (CAr), 129.3 (3xCAr), 134.0 (Cq), 136.5 (Cq), 138.0 (Cq), 142.2 (Cq), 152.7 (2xCAr), 161.1 (C=O) ppm; HRMS (ESI$^+$) m/z calcd for $[C_{33}H_{38}N_6O_4]+H^+$ 597.7271, found 597.7280 $([C_{33}H_{38}N_6O_4]+H)^+$.

***N*-(4-Methyl-3-(pyrazin-2-ylamino)phenyl)-4-((4-(pyrimidin-2-yl)piperazin-1-yl)methyl)benzamide (7):**Yellowish gummy solid (This compound was purified by flash column chromatography using DCM/MeOH 10:1 as eluent, Rf: 0.60 (10:1 DCM/MeOH), yield 50.8%, m.p.143°C; IR (ATR) n_{max} 3291 (br) (NH), 2919 (m), 2812 (w), 1651 (s) (C=O), 1583 (vs), 1546 (s), 1493 (vs), 1445 (s), 1142 (w), 1005 (m) cm^{-1}; ^{1}H NMR (500 MHz, $CDCl_3$): δ = 2.39 (s, 3H, CH_3), 2.53 (brds, 4H, N-CH_2), 3.52 (s, 2H, CH_2), 3.86 (brds, 4H, N-CH_2), 6.50 (t, J= 4.6 Hz, 1H, Ar-H), 7.21 (d, J=8.2 Hz, 2H, Ar-H), 7.28 (brds, 1H, NH), 7.48 (m, 5H, Ar-H), 7.83 (d, J= 7.7 Hz, 2H, Ar-H), 7.91 (s, 1H, ArH), 7.95 (brds, 1H, NH), 8.31 (d, J= 4.6 Hz, 2H, Ar-H) ppm; ^{13}C NMR (125 MHz, $CDCl_3$): δ= 22.3 (CH_3), 43.7 (2xCH_2), 53.0 (2xCH_2), 62.6 (CH_2), 109.9 (CAr), 119.2 (2xCAr), 123.9 (2xCAr), 124.8 (Cq), 127.1 (2xCAr), 129.4 (2xCAr), 130.8 (2xCAr), 133.5 (Cq), 133.9 (2xCq), 136.8 (Cq), 142.5 (Cq), 157.7 (2xCAr), 161.6 (Cq), 165.5 (C=O) ppm; HRMS (ESI$^+$) m/z calcd for $[C_{27}H_{28}N_8O]+H^+$ 481.5722, found 481.3640 $([C_{27}H_{28}N_8O]+H)^+$

***N*-(4-Methyl-3-((4-methylpyrimidin-2-yl)amino)phenyl)-4-(morhpolinomethyl)benzamide (8):** Cream-white gummy solid (This compound was purified by flash column chromatography using DCM/MeOH 10:1 as eluent, Rf: 0.40 (10:1 DCM/MeOH), yield 54.8%, m.p.157°C); IR (ATR): n= 3286 (br) (NH), 3084 (w), 2922 (m), 2854 (m), 1711 (s) (C=O), 1261 (m), 1006 (w) cm^{-1}. ^{1}H NMR (500 MHz, $CDCl_3$): δ = 2.32 (s, 3H, CH_3), 2,38 (s, 3H, CH_3), 2.52 (brds, 4H, N-CH_2), 3.62 (s, 2H, CH_2), 3.98 (t, J= 2.2 Hz, 4H, O-CH_2), 4.03 (brds, 1H, NH), 6.93 (d, J= 2.8 Hz, 1H, ArH), 7.20 (d, J= 3.2 Hz, 1H, Ar-H), 7.48-7.53 (m, 3H, Ar-H), 7.84 (d, J= 4.2 Hz, 2H, Ar-H), 7.92 (s, 1H, ArH), 7.97 (brds, 1H, NH), 8.36 (d, J= 2.8 Hz, 1H, ArH) ppm; ^{13}C NMR (125 MHz, $CDCl_3$): δ = 22.3 (CH_3), 25.9 (CH_3), 43.5 (N-CH_2), 53.6 (N-CH_2), 62.4 (O-CH_2), 62.6 (CH_2), 66.6 (O-CH_2),

110.2 (CAr), 119.1 (CAr), 123.86 (CAr), 124.8 (Cq), 127.2 (3xCAr), 129.6 (2xCAr), 130.7 (CAr), 133.5 (Cq), 133.9 (Cq), 136.7 (Cq), 156.3 (Cq), 165.3 (Cq), 165.5 (C=O), 168.4 (Cq) ppm; HRMS (ESI+) m/z calcd for $C_{24}H_{27}N_5O_2$ 418.2243, found 418.1865 $[C_{24}H_{27}N_5O_2]+H]^+$

***N*-(4-Methyl-3-((4-methylpyridin-2-yl)amino)phenyl)-4-(morhpolinomethyl)benzamide (9):** Cream-white gummy solid, (This compound was purified by flash column chromatography using DCM/MeOH 7:1 as eluent, Rf: 0.60 (7:1 DCM/MeOH), yield 49.4%, m.p.155-157°C); IR (ATR) n_{max} 3292 (br) (NH), 2919 (m), 2852 (m), 1652 (s) (C=O), 1605 (vs), 1563 (m), 1524 (m), 1417 (w), 1261 (m), 1112 (vs), 1006 (vs), 865 (vs), 801 (vs) cm^{-1}; ^1H NMR (500 MHz, $CDCl_3$): δ = 2.33 (s, 3H, CH_3), 2,38 (s, 3H, CH_3), 2.52 (t, J= 2.2 Hz, 4H, N-CH_2), 3.65 (s, 2H, CH_2), 3.98 (t, J= 2.2 Hz, 4H, O-CH_2), 4.00 (brds, 1H, NH), 6.54 (d, J= 4.1 Hz, 1H, ArH), 6.90 (d, J= 2.8 Hz, 1H, ArH), 7.20 (d, J= 3.2 Hz, 1H, Ar-H), 7.48-7.53 (m, 3H, Ar-H), 7.88 (d, J= 4.2 Hz, 2H, Ar-H), 7.90 (s, 1H, ArH), 7.99 (brds, 1H, NH), 8.32 (d, J= 2.8 Hz, 1H, ArH) ppm; ^{13}C NMR (125 MHz, $CDCl_3$): δ = 22.3 (CH_3), 25.7 (CH_3), 42.4 (N-CH_2), 55.92 (N-CH_2), 62.4 (O-CH_2), 63.9 (CH_2), 68.5 (O-CH_2), 109.0 (CAr), 110.3 (CAr), 119.4 (CAr), 123.9 (CAr), 125.0 (Cq), 126.9 (3xCAr), 129.5 (2xCAr), 130.8 (CAr), 133.6 (Cq), 133.8 (Cq), 136.5 (Cq), 156.0 (Cq), 165.4 (Cq), 165.5 (C=O), 168.4 (Cq) ppm; HRMS (ESI^+) m/z calcd for $[C_{25}H_{28}N_4O_2]+H^+$ 417.5234, found 417.5270 $([C_{25}H_{28}N_4O_2]+H)^+$.

***N*-(4-Methyl-3-((4-methylpyridin-2-yl)amino)phenyl)-4-((4-(2,3,4-trimethoxybenzyl)piperazin-1-yl)methyl)benzamide (10):**

Orange-brownish gummy solid, (This compound was purified by flash column chromatography using DCM/MeOH 7:1 as eluent, Rf: 0.54 (7:1 DCM/MeOH), yield 44.6%, m.p.87°C); IR (ATR) n_{max} 3295 (NH), 2936, 2811, 1652 (C=O), 1140, 1008 cm^{-1}; ^1H NMR (500 MHz, $CDCl_3$): δ = 2.24 (s, 3H, CH_3), 2.41 (s, 3H, CH_3), 2.53 (brds, 8H, N-CH_2), 3.45 (s, 2H, CH_2), 3.54 (s, 2H, CH_2), 3.85 (s, 3H, O-CH_3), 3.86 (s, 3H, O-CH_3), 3.88 (s, 3H, O-CH_3), 6.49 (d, J= 5.0 Hz, 1H, Ar-H), 6.59 (d, J= 5.0 Hz, 1H, Ar-H), 6.62 (d, J= 8.5 Hz, 1H, Ar-H), 6.92 (brds, 1H, NH), 7.01 (d, J= 8.5 Hz, 1H, Ar-H), 7.16 (d, J=8.3 Hz, 1H Ar-H), 7.40 (d, J=8.1 Hz, 1H, Ar-H), 7.44 (d, J=7.3 Hz, 2H, Ar-H), 7.79 (d, J= 8.1 Hz, 2H, Ar-H), 8.03 (brds, 1H, NH), 8.26 (d, J= 5.0 Hz, 1H, Ar-H), 8.33 (d, J= 1.9 Hz, 1H, Ar-H) ppm; ^{13}C NMR (125 MHz, $CDCl_3$): δ = 20.6 (CH_3), 24.1(CH_3), 53.0 (2xN-CH_2), 55.9 (OCH_3), 56.3 (2xCH_2), 60.3 (OCH_3), 61.1 (OCH_3), 62.5 (2xN-CH_2) 106.9 (CAr), 109.8 (CAr), 112.3 (CAr), 112.7 (CAr), 114.9 (CAr), 123.5 (Cq), 125.3 (CAr), 127.0 (3xCAr), 129.3 (2xCAr), 130.8 (CAr), 134.0 (Cq), 136.5 (Cq), 138.0 (Cq), 142.2 (Cq), 142.4 (Cq), 150.2 (2xCq), 157.4 (CAr), 160.1 (Cq), 165.5 (Cq), 168.3 (C=O) ppm; HRMS (ESI+) m/z calcd for $[C_{35}H_{41}N_5O_4]+H^+$ 596.7391, found 596.7520 $([C_{35}H_{41}N_5O_4]+H)^+$.

Biological assays

Cell Culture

K562, Jurkat, Molt-4, and Nalm-6 cell lines were cultured in RPMI medium (ECM2001, Euroclone), REH cell line was cultured in DMEM medium (LM-D1111- Biosera) Hek293T cell line was cultured in IMDM medium (AL070A - HiMedia) supplemented with 10% heat inactivated fetal bovine serum (F7524-Merck &

Co., USA,) penicillin and streptomycin (P4333-Sigma Aldrich). K562, Jurkat and Molt-4 cell lines were seeded as $4x10^5$/ml, REH and Nalm-6 cell lines were seeded $5x10^5$/ml, Hek293T cell line was seed as $2x10^5$/ml. All cells were incubated at 5% CO_2 and 37 °C. All cell lines were kindly provided by Dr. M. Sayitoglu and Dr. Ö. Hatirnaz-Ng from Acibadem University.

In vitro toxicity assay

MTT assay [67] was used to evaluate the growth inhibition percentage of the newly synthesized imatinib compounds against different types of leukemia cell lines (K562, Nalm-6, Molt4, REH and Jurkat) and control cell line non-leukemia cell line (Hek293T).

MTT assay is a 3-day test. On the first day, cell count was performed in Bio Rad TC-20 device with the help of trypan blue, each cell line was prepared by diluting to the specified concentrations and seeded in a 96-well plate as 100µL to each well and incubated for 1 day.

Each compound was solved in DMSO, their stock solutions (33.3, 10, 5, 1, mM and 300 µM) were prepared by diluting with the same solvent and they stored under -20°C when they were not used.

On the second day, stock solutions were subsequently diluted to various concentrations (0.3-200 µM) with related medium prior to experiments. Specified concentrations of the compounds were seeded in a 96-well plate as 100µL to each well and incubated for 24 hours.

After incubation (on the third day), to precipitate leukemia cells, the cell plate was centrifuged at 1500 rpm for 5 minutes. Then, 100 µl of supernatant was removed from each well carefully and 10 µl of MTT solution (5 mg/mL) was added to each well and incubated at 37 °C for 4 hours. The 50 µl of supernatant was discarded from each well and 100 µl of DMSO was added to dissolve the formazan. Plates were shaken for 45 minutes to dissolve the dye. Then the optical density of each well was measured by using Thermo VarioSkan Flush Multimode Reader Quantum ST5-1100 at 570 nm wavelength. The IC_{50} values were calculated by using GraphPad Prism.

Subsequently, inhibition percentage of the cells was determined by following formula

(Inhibition rate (%) = $[(OD_{(control)}-OD_{(sample)}]/OD_{(control)}$ x100).

OD = Optical Density

Statistical Analyses for IC_{50}

All the data presented as the mean of 6 replicates. Results were analyzed and illustrated with Graph Pad Prism (version 5; GraphPad Software, San Diego, CA, USA). Statistical analysis was performed using dose-response inhibition, log(inhibitor) vs response-variable slope, least squares (ordinary) fit.

ABL1 Expression analysis

Raw data generated using Affymetrix Human Gene 1.0 ST Array were collected from Gene Expression Omnibus (GEO) using the accession numbers GSE139094 (Hek293T), GSE48558 (Jurkat, K562, Nalm-6 and REH) and GSE26790 (Molt-4). The raw data were processed using the Robust Multi-array Average (RMA) method, which is part of the R package oligo [71] and the batch effect was removed using the limma package [72]. The Affymetrix Probe IDs were mapped to Ensembl IDs with the help of hugene10sttranscriptcluster.db annotation package in R. The normalized and log2-transformed expression values for the gene ABL1 were extracted using the Ensembl ID ENSG0000097007. To assess whether difference exists in expression level of ABL1 among the cell lines we performed one-way analysis of variance (ANOVA) assuming unequal variances.

Molecular docking

Prediction of Target Protein

Putative targets for the newly synthesized imatinib analogs were predicted using Similarity Ensemble Approach (SEA, www.sea.bkslab.org) online search tool provided by Shoichet Laboratory in the Department of Pharmaceutical Chemistry at the University of California [49]. For this, SMILES representations for the derivatives were generated and used as search keys to the SEA server that uses chemical similarity to find protein targets.

Crystal Structures and Docking Procedure

In order to assess which conformation of ABL1 and BRAF kinases our newly synthesized compounds bind to, we performed molecular docking simulations using 8 and 7 different crystal structures of kinase domains of wild type ABL1 and BRAF respectively. The properties of the structures used in this study together with the original ligands that are bound to the structures are given in Table S4 and Table S6.

We used the chemical toolbox Open Babel 2.4.167 in order to build the initial conformations of the compounds from their SMILES representations. The target protein structures (see Table S5) and compounds were prepared for docking using the AutoDock Tools version 1.5.6 [69]. AutoTors utility of AutoDock Tools was used for definition of the torsions of the compounds. All torsions except for amide and ring torsions were treated as flexible. Gasteiger atomic charges [70] were assigned to both the protein and the compounds. The non-polar hydrogen atoms were merged while the polar hydrogen atoms were kept explicit.

Extensive docking simulations were performed using the program AutoDock 4.2 [69]. Grid maps were generated with 0.375Å spacing by the AutoGrid program. The grid center was chosen to coincide with the center of the original ligand in the crystal structure. Grid dimensions (70Å x 70Å x 70Å) that span the binding pocket in three dimensions were computed.

Standard Lamarckian genetic algorithm protocol was used with default settings, except for the number of energy evaluations and the number of independent runs, which were increased to obtain more reliable results. We started molecular docking simulations with 25 million energy evaluations for imatinib and its

newly synthesized 6 analogs. We assessed the convergence of a docking simulation by performing clustering analysis of the resulting docking conformations where we used a root mean square deviation of 2 Å as cut-off. We assumed that the docking simulation was converged when 20 % of the 100 independent runs resulted in the same binding conformation. When this condition was not met, we increased the maximum number of energy evaluations gradually. Due to their relatively high number of torsions (10 for compound 6 and 11 for compound 10), we performed additional docking simulations for the compounds 6 and 10 where we set the maximum number of energy evaluations to 30, 40 and 50 million. For the docking simulations of imatinib, Compound 5, Compound 7, Compound 8 and Compound 9; 25 million of maximum number of energy evaluations sufficed. However, for all reported results, a maximum number of energy evaluations of 40 million was used. The starting point of the ligand was generated randomly, in all docking simulations

Declarations

Acknowledgements

We would like to offer special thanks to Prof. Dr. Nuket Ocal, who, although no longer with us, for her valuable contribution to this project. This study was supported by the Research Fund of Yildiz Technical University (Project Number: FYL-2017-3173).

Conflict of Interest

The authors declared that there are no conflicts of interest.

References

1. 1. Tuglu MM, Melli M. Imatinib: Mechanisms of Action and Mechanisms of Resistance Development. J Ankara Univ Fac Med. 2012;65(2):77-82 doi: 10.1501/Tıpfak_000000813.
2. Xia ZL, Mo Y,Yu YJ, Chong BH. PDGFR Inhibitor Imatinib May be a Potent Drug in Treating Essential Thrombocythemia. Blood. 2016; 128(22): 5470. doi:10.1182/blood.V128.22.5470.5470.
3. Rossari F, Minutolo F and Orciuolo E. Past, present, and future of Bcr-Abl inhibitors: from chemical development to clinical efficacy. J. Hematol. Oncol. 2018; 11:84. doi:10.1186/s13045-018-0624-2.
4. (a) Zimmermann, J, inventor; Pyrimidine derivatives and processes for their preparation. EP Patent PT564409E, 1993 March 25.
   (b) Zimmermann, J, inventor; Pyrimidine derivatives and processes for the preparation thereof. U.S. Patent 5,521,184A. 1996 May 28.

   (c) Zimmermann J, Buchdunger E, Mett H, Meyer T, Lydon NB, Traxler P. (Phenylamino)pyrimidine (PAP) derivatives: a new class of potent and highly selective PDGF-receptor autophosphorylation inhibitors. Bioorg Med Chem Lett. 1996; 6: 1221–1226. doi: 10.1016/0960-894X(96)00197-7.

5. Kompella A, Bhujanga Rao AKS, Venkaiah Chowdary NWO. A Facile Total Synthesis for Large-Scale Production of Imatinib Base Org. Process Res. Dev. 2012;16(11):1794–1804. doi: 10.1021/op300212u.
6. Szczepek W, Luniewski W, Kaczmarek L, Zagrodzki B, Lazinska DS, Szelejewski W, Skarzynski M, inventors; Process for preparation of imatinib base. World Pat., 2006071130, 2006 July 06.
7. Loiseleur O, Kaufmann D, Abel S, Buerger HM, Meisenbach M, Schmitz B, Sedelmeier G, inventors; Process for the preparation of imatinib base. W.O.Patent 03/066,613, 2003 August 14.
8. Zhang X, Sun J, Chen T, Yang C, Yu L. A Practical Preparation of Imatinib Base. Synlett. 2016; 27: 2233-2236. doi: 10.1055/s-0035-1562498.
9. Kang J, Lee JY, Park JH, Chang DJ. Synthesis of imatinib, a tyrosine kinase inhibitor, labeled with carbon-14. J.Label Compd Radiopharm. 2020;63:174–182. doi:10.1002/jlcr.3830
10. Macdonald P, Rossetto P, inventors; Process for the preparation of imatinib. World Pat. 2008051597, 2008 May 02.
11. Xing L, Xungui H, Wang Y, Bekhazi M, Krivonos S, Danon E, inventors; Imatinib production process. World Pat. 2008135980, 2008 November 13.
12. Ivanov S, Shishkov SV. Synthesis of imatinib: a convergent approach revisited. Monatsh. Chem., 2009;140, 619–623. doi:10.1007/s00706-008-0105-3.
13. Zhao Y, Li Z, Liu G, Liu C, Xu L, inventors; Method for preparing imatinib. Chinese Pat., 101921260, 2013 Jan 16.
14. Yan R, Yang H, Hou W, Xu Y, inventors; Convenient and quick method for preparing high-purity imatinib and mesylate thereof. Chinese Pat. 101985442, 2011 March 16.
15. Kamath GG, Pai AM, Ujagare X, He S, Wu X, Shen JY, Zhan H, inventors; Process for the preparatıon of ımatınıb and salts thereof. World Pat. 2011070588, 2011 June 16.
16. Hopkin MD, Baxendale IR, Ley SV. A flow-based synthesis of Imatinib: the API of Gleevec. Chem. Commun. 2010;14. doi:10.1039/C001550D.
17. Hopkin,MD, BaxendaleIR, Ley SV. An expeditious synthesis of imatinib and analogues utilising flow chemistry methods. Org. Biomol. Chem. 2013;11. doi: 10.1039/C2OB27002A.
18. Zhang X, Sun J, Chen T, Yang C and Yu L. A Practical Preparation of Imatinib Base. Synlett. 2016; 27(15), 2233. doi:10.1055/s-0035-1562498.
19. Ingham RJ, Riva E, Nikbin N, Baxendale IR, Ley SV. A “Catch–React–Release” Method for the Flow Synthesis of 2-Aminopyrimidines and Preparation of the Imatinib Base. Org. Lett. 2012;14, 3920–3923. doi: 10.1021/ol301673q.
20. Leonetti F, Capaldi C, Carotti A. Microwave-assisted solid phase synthesis of Imatinib, a blockbuster anticancer drug. Tetrahedron Lett. 2007;48, 3455–3458. doi: 10.1016/j.tetlet.2007.03.033.
21. Heo Y, Hyun D, Kumar MR, Jung HM, Lee S. Preparation of copper(II) oxide bound on polystyrene beads and its application in the aryl aminations: synthesis of Imatinib. Tetrahedron Letters. 53 2012;49, 6657–6661. doi: 10.1016/j.tetlet.2012.09.097.

22. Lee SH, Ryu JC, El-Deeb IM. Synthesis of new N-arylpyrimidin-2-amine derivatives using a palladium catalyst. Molecules. 2008; 13(4): 818–830. doi: 10.3390/molecules13040818.
23. Fors BP, Watson DA, Biscoe MR, Buchwald SL. A Highly Active Catalyst for Pd-Catalyzed Amination Reactions: Cross-Coupling Reactions Using Aryl Mesylates and the Highly Selective Monoarylation of Primary Amines Using Aryl Chlorides. J. Am. Chem. Soc. 2008; 130, 13552-13554. doi:10.1021/ja8055358.
24. Maiti D, Fors BP, Henderson JL, Nakamura Y, Buchwald SL. Palladium-catalyzed coupling of functionalized primary and secondary amines with aryl and heteroaryl halides: two ligands suffice in most cases. Chem. Sci. 2011; 2, 57. doi:10.1039/C0SC00330A.
25. Hubbard SR. Autoinhibitory mechanisms in receptor tyrosine kinases. Front. Biosci. 2002; 1(7), 330-340. doi:10.2741/hubbard.
26. Paul MK and Mukhopadhyay AK. Tyrosine kinase - Role and significance in Cancer. Int J. Med. Sci. 2004, 1(2), 101. doi: 10.7150/ijms.1.101.
27. Madhusudan S, Ganesan T. Tyrosine kinase inhibitors in cancer therapy. Clin. Biochem. 2004; 37: 618–635. doi: 10.1016/j.clinbiochem.2004.05.006.
28. Bhullar KS, Lagaron NO, McGowan EM, Parmar I, Jha A, Hubbard BP, Rupasinghe HPV. Kinase-targeted cancer therapies: progress, challenges and future directions. Mol. Cancer. 2018; 17:48. doi:10.1186/s12943-018-0804-2.
29. Yaghmaie M, Yeung CCS. Molecular Mechanisms of Resistance to Tyrosine Kinase Inhibitors. Curr. Hematol. Malig. Rep. 2019; 14:395–404. doi:10.1007/s11899-019-00543-7.
30. Bitencourt R, Zalcberg I, Louro ID. Imatinib resistance: a review of alternative inhibitors in chronic myeloid leukemia. Rev Bras Hematol Hemoter. 2011; 33(6): 470-475. doi:10.5581/1516-8484.20110124.
31. Huang M, Dorsey JF, Epling-Burnett PK, Nimmanapalli R, Landowski TH, Mora LB, Niu G, Sinibaldi D, Bai F, Kraker A. et al. Inhibition of Bcr-Abl kinase activity by PD180970 blocks constitutive activation of Stat5 and growth of CML cells. Oncogene. 2002; 21, 8804. doi:10.1038/sj.onc.1206028.
32. Warmuth M, Simon N, Mitina O, Mathes R, Fabbro D, Manley PW, Buchdunger E, Forster K, Moarefi I, Hallek M. Dual-specific Src and Abl kinase inhibitors, PP1 and CGP76030, inhibit growth and survival of cells expressing imatinib mesylate-resistant Bcr-Abl kinases. Blood .2003; 101, 664. doi:10.1182/blood-2002-01-0288.
33. Shah NP, Tran C, Lee FY, Chen P, Norris D, Sawyers CL. Overriding Imatinib Resistance with a Novel ABL Kinase Inhibitor. Science. 2004; 305, 399. doi:10.1126/science.1099480.
34. Weisberg E, Manley P, Mestan J, Cowan-Jacob S, Ray A, Griffin JD. AMN107 (nilotinib): a novel and selective inhibitor of BCR-ABL. J. Cancer. 2006; 94(12), 1765. doi:10.1038/sj.bjc.6603170.
35. O'Hare T, Shakespeare WC, Zhu X, et al. AP24534, a pan-BCR-ABL inhibitor for chronic myeloid leukemia, potently inhibits the T315I mutant and overcomes mutation-based resistance. Cancer Cell. 2009; 16(5):401-412. doi:10.1016/j.ccr.2009.09.028.

36. Hoover RR, Mahon FX, Melo JV, Daley GQ. Overcoming STI571 resistance with the farnesyl transferase inhibitor SCH66336. Blood. 2002; 100:1068-71. doi:10.1182/blood.v100.3.1068.
37. Manley PW, Stiefl N, Cowan-Jacob SW, Kaufman S, Mestan J, Wartmann M, Wiesmann M, Woodman R, Gallagher N. Structural resemblances and comparisons of the relative pharmacological properties of imatinib and nilotinib. Bioorg. Med. Chem. 2018; 26(15), 4537-43. doi:10.1016/j.bmc.2010.08.026.
38. Kumar S, Deep A, Narasimhan B. A Review on Synthesis, Anticancer and Antiviral Potentials of Pyrimidine Derivatives. Curr. Bioact. Compd. 2019; 15(3):289-303. doi:10.2174/1573407214666180124160405.
39. Jahandideh S, Maghsood F, Ghahhari NM, Lotfinia M, Mohammadi M, Johari B, Kadivara M. The effect of Trimetazidine and Diazoxide on immunomodulatory activity of human embryonic stem cell-derived mesenchymal stem cell secretome. Tissue Cell. 2017; 49(5):597-602. doi:10.1016/j.tice.2017.08.003.
40. Gatta L, Vitiello L, Gorini S, Chiandotto S, Costelli P, Giammarioli AM, Malorni W, Rosano G, Ferraro E. Modulating the metabolism by trimetazidine enhances myoblast differentiation and promotes myogenesis in cachectic tumorbearing c26 mice. Oncotarget. 2017;8(69):113938-113956. doi:10.18632/oncotarget.23044.
41. Aubry S, Pellet-Rostaing S, dit Chabert JF, Ducki S, Lemaire M. Synthesis and inhibition of cancer cell proliferation of (1,3')-bis-tetrahydroisoquinolines and piperazine systems. Bioorg. Med. Chem. Lett. 2007; 17(9):2598-2602. doi:10.1016/j.bmcl.2007.01.108.
42. Mistry B, Keum YS and Kim DH. Synthesis and Biological Evaluation of Berberine Derivatives Bearing 4-Aryl-1-Piperazine Moieties. J. Chem. Res. 2015, 39, 470. doi: 10.3184/174751915X14381686689721.
43. Ma Y, Zheng X, Gao H, Wan C, Rao G and Mao Z. Design, Synthesis, and Biological Evaluation of Novel Benzofuran Derivatives Bearing N-Aryl Piperazine Moiety. Molecules. 2016, 21, 1684. doi:10.3390/molecules21121684.
44. Su H, Xue Z, Feng Y, Xie Y, Deng B, Yao Y, Tian X, An Q, Yang L, Yao Q, Xue J, Chen G, Hao C, Zhou T. N-arylpiperazine-containing compound (C2): An enhancer of sunitinib in the treatment of pancreatic cancer, involving D1DR activation. Toxicol. Appl. Pharmacol. 2019, 384, 114789. doi:10.1016/j.taap.2019.114789.
45. Jakubowska J, Wasowska-Lukawska M and Czyz M. STI571 and morpholine derivative of doxorubicin collaborate in inhibition of K562 cell proliferation by inducing differentiation and mitochondrial pathway of apoptosisM, Eur. J. Pharmacol. 2008, 596(1–3), 41. doi:10.1016/j.ejphar.2008.08.021.
46. Hamidian H, Aziz S. Synthesis of novel compounds containing morpholine and 5(4H)-oxazolone rings as potent tyrosinase inhibitors. Bioorg. Med. Chem. 2015; 23(21), 7089-7094. doi: 10.1016/j.bmc.2015.09.015.
47. Goud NS, Pooladanda V, Mahammad GS, et.al. Synthesis and biological evaluation of morpholines linked coumarin–triazole hybrids as anticancer agents. Chem Biol Drug Des. 2019; 94:1919–1929.

doi: 10.1111/cbdd.13578.

48. https://www.molinspiration.com
49. Keiser MJ, Roth BL, Armbruster BN, Ernsberger P, Irwin JJ, Shoichet BK. Relating protein pharmacology by ligand chemistry. Nat Biotech. 2007; 25 (2), 197-206. doi:10.1038/nbt1284.
50. Manley PW, Cowan-Jacob SW, Buchdunger E, Fabbro D, Fendrich G, Furet P, Meyer T, Zimmermann J. Imatinib: a selective tyrosine kinase inhibitor. Eur. J. Cancer. 2002; 38: S19-S27. doi:10.1016/s0959-8049(02)80599-8.
51. Levinson NM, Kuchment O, Shen K, Young MA, Koldobskiy M, Karplus M, Cole PA, Kuriyan J. A Src-like inactive conformation in the Abl tyrosine kinase domain. Plos Biology, 2006; 4(5), 753-767. doi:10.1371/journal.pbio.0040144.
52. Cowan-Jacob SW, et al. Structural biology contributions to the discovery of drugs to treat chronic myelogenous leukaemia. Acta Cryst. D. 2007; 63, 80-93. doi:10.1107/S0907444906047287.
53. Bernstein FC, et al. Protein Data Bank - Computer-Based Archival File For Macromolecular Structures. J. Mol. Biol. 1977; 112(3):535-542. doi:10.1016/0003-9861(78)90204-7.
54. Berman HM, et al. The Protein Data Bank. Nucleic Acids Res. 2000; 28(1): 235-242. doi:10.1093/nar/28.1.235.
55. Horio T, et al. Structural factors contributing to the Abl/Lyn dual inhibitory activity of 3-substituted benzamide derivatives. Bioorg. Med. Chem. Lett. 2007; 17(10):2712-2717. doi:10.1016/j.bmcl.2007.03.002.
56. Weisberg E, et al. Characterization of AMN107, a selective inhibitor of native and mutant Bcr-Abl. Cancer Cell. 2005; 7(2):129-141. doi:10.1016/j.ccr.2005.01.007.
57. Levinson NM, Boxer SG. Structural and Spectroscopic Analysis of the Kinase Inhibitor Bosutinib and an Isomer of Bosutinib Binding to the Abl Tyrosine Kinase Domain. Plos One. 2012; 7(4). doi:10.1371/journal.pone.0029828.
58. Jensen CN, et al. Structures of the Apo and FAD-Bound Forms of 2-Hydroxybiphenyl 3-monooxygenase (HbpA) Locate Activity Hotspots Identified by Using Directed Evolution. Chembiochem. 2015; 16(6):968-976. doi:10.1002/cbic.201402701.
59. Laskowski RA, Swindells MB. LigPlot+: multiple ligand-protein interaction diagrams for drug discovery. J. Chem. Inf. Model. 2011; 51(10):2778-86. doi:10.1021/ci200227u.
60. Wan PTC, et al. Mechanism of activation of the RAF-ERK signaling pathway by oncogenic mutations of B-RAF. Cell. 2004;116(6):855-867. doi:10.1016/s0092-8674(04)00215-6.
61. Okaniwa M, et al. Discovery of a Selective Kinase Inhibitor (TAK-632) Targeting Pan-RAF Inhibition: Design, Synthesis, and Biological Evaluation of C-7-Substituted 1,3-Benzothiazole Derivatives. J. Med. Chem. 2013; 56(16):6478-6494. doi:10.1021/jm400778d.
62. Lavoie H, et al. Inhibitors that stabilize a closed RAF kinase domain conformation induce dimerization. Nat. Chem. Biol. 2013; 9(7): 428-436. doi:10.1038/nchembio.1257.

63. Tsai J, et al. Discovery of a selective inhibitor of oncogenic B-Raf kinase with potent antimelanoma activity. Proc. Natl. Acad. Sci. 2008; 105(8):3041-3046. doi:10.1073/pnas.0711741105.
64. Waizenegger IC, et al. A Novel RAF Kinase Inhibitor with DFG-Out-Binding Mode: High Efficacy in BRAF-Mutant Tumor Xenograft Models in the Absence of Normal Tissue Hyperproliferation. Mol. Cancer Ther. 2016; 15(3):354-365. doi:10.1158/1535-7163.MCT-15-0617.
65. King AJ, et al. Demonstration of a genetic therapeutic index for tumors expressing oncogenic BRAF by the kinase inhibitor SB-590885. Cancer Res. 2006; 66(23):11100-11105. doi:10.1158/0008-5472.CAN-06-2554.
66. Hansen JD, et al. Potent and selective pyrazole-based inhibitors of B-Raf kinase. Bioorg. Med. Chem. Lett. 2008; 18(16):4692-4695. doi:10.1016/j.bmcl.2008.07.002.
67. Cory AH, Owen TC, Barltrop JA, Cory JG. Use of an aqueous soluble tetrazolium/formazan assay for cell growth assays in culture. Cancer Commun. 1991; 3(7):207-12. doi: 10.3727/095535491820873191.
68. O'Boyle NM, et al. Open Babel: An open chemical toolbox. J. Cheminformatics. 201; 3. doi:10.1186/1758-2946-3-33.
69. Morris GM, et al. AutoDock4 and AutoDockTools4: Automated Docking with Selective Receptor Flexibility. J. Comput. Chem. 2009; 30(16): 2785-2791. doi:10.1002/jcc.21256.
70. Gasteiger J, Marsili MA new model for calculating atomic charges in molecules. Tetrahedron Lett. 1978; 19(34):3181-3184. doi:10.1016/S0040-4039(01)94977-9.
71. Carvalho BS, Irizarry RA. A framework for oligonucleotide microarray preprocessing. Bioinformatics. 2010;26(19):2363-7. doi:10.1093/bioinformatics/btq431.
72. Ritchie ME, Phipson B, Wu D, Hu Y, Law CW, Shi W, et al. limma powers differential expression analyses for RNA-sequencing and microarray studies. Nucleic Acids Res. 2015;43(7):e47. doi:10.1093/nar/gkv007.

Tables

Table1.The chemical structures, IC_{50} values (μM) and maximum inhibition rate (efficacy) (%) of the compounds 5-10 against K562, Nalm6, Molt4, REH, Jurkat, HEK293T

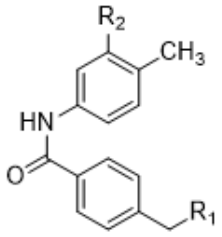

Comp.	R^1	R^2		K562[a]	Nalm-6[b]	Molt-4[b]	REH[b]	Jurkat[b]	Hek293T[c]
5	A	D	Efficacy (%)	6.48	30.08	25.17	25.24	33.54	50.92
			IC_{50}	>200	>200	>200	>200	>200	8.756
6	B	D	Efficacy (%)	32.46	59.14	44.84	38.85	64.70	55.35
			IC_{50}	>200	47.96	>200	>200	49.91	20.63
7	A	E	Efficacy (%)	40.50	40.27	16.40	37.22	31.25	44.89
			IC_{50}	>200	>200	>200	>200	>200	>200
8	C	D	Efficacy (%)	39.64	29.23	23.36	15.88	33.87	41.83
			IC_{50}	>200	>200	>200	>200	>200	>200
9	C	F	Efficacy (%)	55.03	60.82	41.42	15.26	60.91	57.22
			IC_{50}	76.73	1.639	>200	>200	85.24	50.65
10	B	F	Efficacy (%)	63.11	72.04	59.99	44.75	63.06	27.16
			IC_{50}	35.40	28.73	33.20	>200	40.06	>200
imatinib[d]	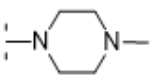	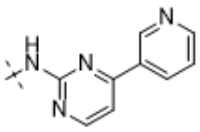	Efficacy (%)	70.29	70.96	79.74	43.03	72.79	58.47
			IC_{50}	78.37	16.09	37.04	>200	12.52	16.73

[a] BCR-ABL positive leukemic cell line. [b] BCR-ABL negative leukemic cell lines. [c] non-leukemic human embryonic kidney tissue. [d] control drug. Percentage of maximum inhibition referred to enzyme activity level treated with different compounds in the range of 0.3-200μM. All experiments were performed in six replicates.

Table2.The results of molecular docking to wild type human ABL1 kinase domain. Binding free energies (ΔG) correspond to the highest-ranking conformation of the largest cluster. The energy values are in

kcal/mol. Number in parenthesis shows the percentage of independent runs that resulted in the same docked conformation. Values depicted in gray correspond to the docking simulations that did not meet our convergence criterion.

Structures	ΔG for compounds (kcal/mol)						
	5	6	7	8	9	10	Imatinib
2HYY[a]	-13.0 (35 %)	-10.1 (15 %)	-13.0 (92 %)	-12.0 (62 %)	-12.1 (98 %)	-14.2 (42 %)	-14.7 (34 %)
2E2B[b]	-13.0 (49 %)	-10.5 (11 %)	-12.8 (90 %)	-11.9 (81 %)	12.1 (96 %)	-13.9 (45 %)	-14.5 (57 %)
2HZ0[c]	-13.6 (43 %)	-9.5 (6 %)	-13.3 (75 %)	-12.4 (64 %)	-12.6 (67 %)	-11.6 (9 %)	-14.6 (78 %)
3CS9[d]	-9.4 (33 %)	-9.6 (12 %)	-12.9 (49 %)	-10.9 (59 %)	-11.3 (79 %)	-12.8 (30 %)	-13.1 (38 %)
3UE4[e]	-9.8 (20 %)	-10.5 (8 %)	-8.2 (13 %)	-9.1 (42 %)	-8.9 (47 %)	-11.2 (21 %)	-10.1 (34 %)
4YC8[f]	-10.1 (15 %)	-10.2 (8 %)	-9.7 (36 %)	-9.0 (35 %)	-8.9 (46 %)	-9.9 (22 %)	-9.6 (25 %)
2HZI[g]	-11.3 (23 %)	-11.8 (20 %)	-11.2 (22 %)	-11.2 (91 %)	-10.1 (38 %)	-11.1 (21 %)	-12.1 (51 %)
2HZ4[h]	-8.7 (15 %)	-11. 0 (12 %)	-9.2 (29 %)	-9.3 (66 %)	-8.8 (39 %)	-9.7 (26 %)	-9.9 (56 %)

[a] Human Abl kinase domain in complex with imatinib. [b] Crystal structure of the c-Abl kinase domain in complex with INNO-406. [c] Abl kinase domain in complex with NVP-AEG082. [d] Human ABL kinase in complex with nilotinib. [e] Structural and spectroscopic analysis of the kinase inhibitor bosutinib binding to the Abl tyrosine kinase domain. [f] C-Helix-Out Binding of Dasatinib Analog to c-Abl Kinase. [g] Abl kinase domain in complex with PD180970. [h] Abl kinase domain unligated and in complex with tetrahydrostaurosporine.

Table3.The results of molecular docking to wild type human BRAF kinase domain. Binding free energies (ΔG) correspond to the highest-ranking conformation of the largest cluster. The energy values are in kcal/mol. Number in parenthesis shows the percentage of independent runs that resulted in the same docked conformation. Values depicted in gray correspond to the docking simulations that did not meet our convergence criterion.

ΔG for compounds (kcal/mol)						
Structures	5	6	7	8	9	10
1UHW[a]	-11.7 (39 %)	-10.7 (11 %)	-12.0 (32 %)	-10.5 (56 %)	-11.2 (76 %)	-11.3 (10 %)
4KSP[b]	-11.1 (10 %)	-9.8 (16 %)	-10.1 (52 %)	-10.0 (45 %)	10.7 (52 %)	-11.5 (20%)
4JVG[c]	-10.8 (56 %)	-8.7 (9 %)	-11.0 (55 %)	-10.2 (27 %)	-9.8 (54 %)	-10.3 (14 %)
3C4C[d]	-8.9 (22 %)	-10.4 (15 %)	-10.2 (20 %)	-7.6 (23 %)	-9.5 (43 %)	-9.5 (24 %)
5C5W[e]	-8.7 (29 %)	-10.8 (16 %)	-11.3 (6 %)	-8.5 (52 %)	-9.6 (86 %)	-11.5 (45 %)
2FB8[f]	-9.7 (35 %)	-8.9 (11 %)	-9.0 (15 %)	-8.7 (42 %)	-8.8 (50 %)	-9.5 (8 %)
3D4Q[g]	-9.3 (24 %)	-9.8 (16%)	-9.5 (13 %)	-9.6 (37 %)	-8.6 (30 %)	-8.4 (13 %)

[a] Solution structure of the DEP domain of mouse pleckstrin. [b] Crystal Structure of Human B-raf bound to a DFG-out Inhibitor TAK-632. [c] B-Raf Kinase in Complex with Birb796. [d] B-Raf Kinase in Complex with PLX4720. [e] 1.25 A resolution structure of an RNA 20-mer. [f] Structure of the B-Raf kinase domain bound to SB-590885. [g] Pyrazole-based inhibitors of B-Raf kinase.

Figures

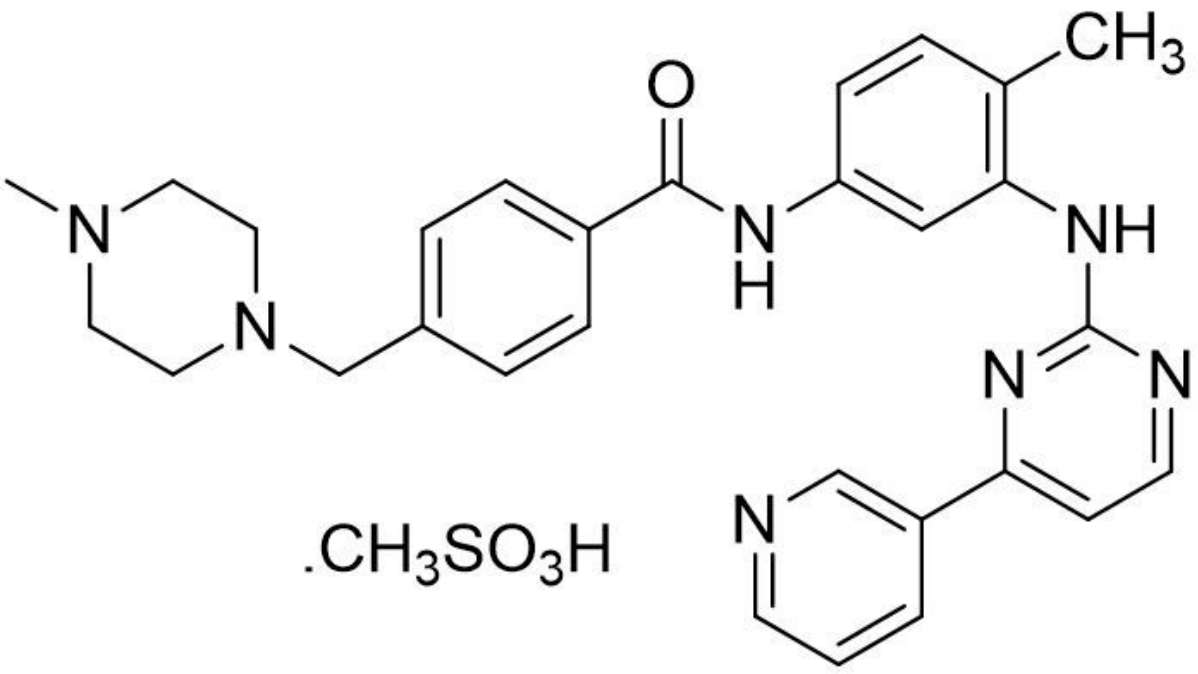

Figure 1

Imatinib mesylate molecular structure.

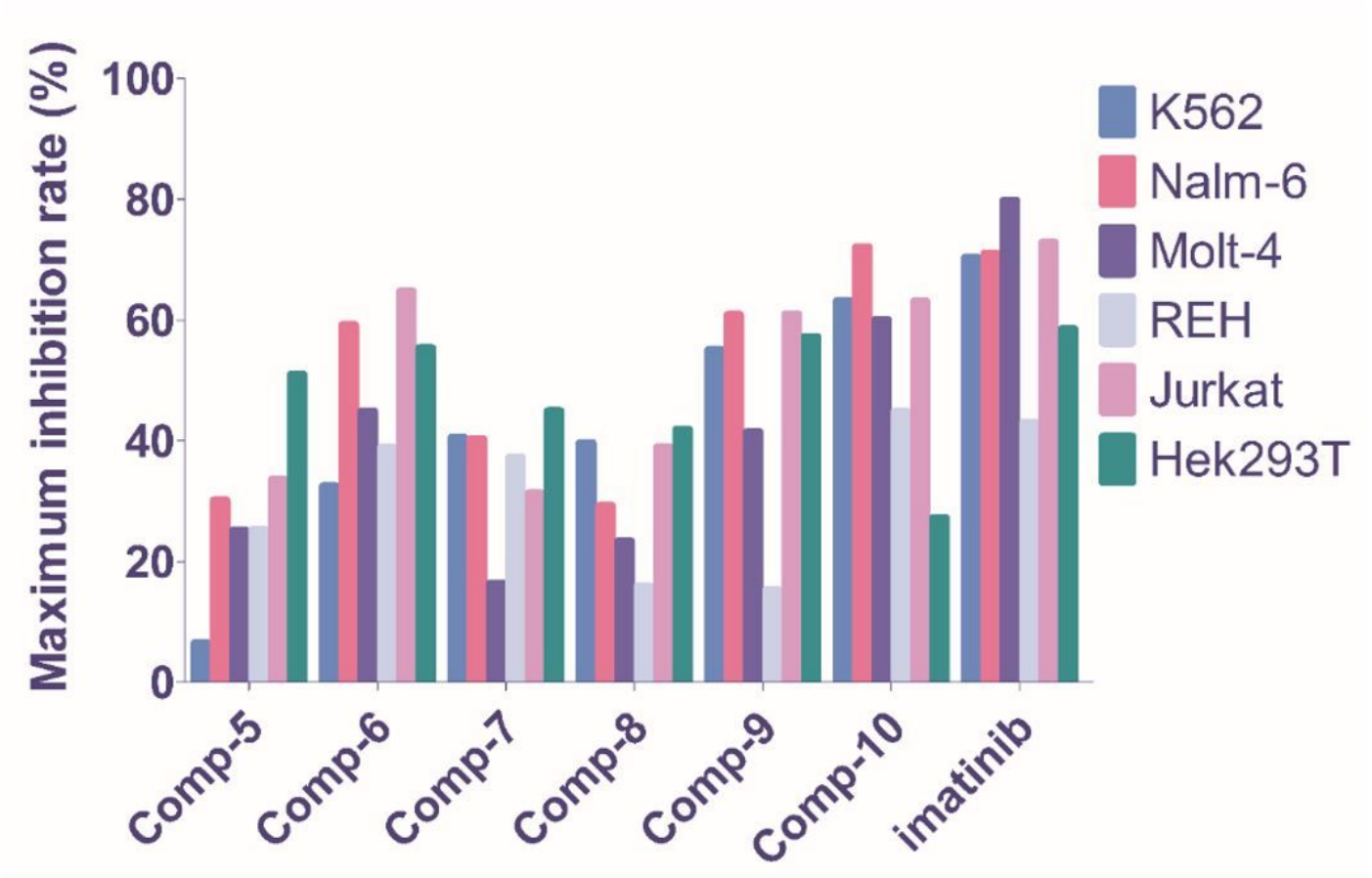

Figure 2

Maximum inhibition rate between 0.3-200μM of the Compound 5-10 and Imatinib.

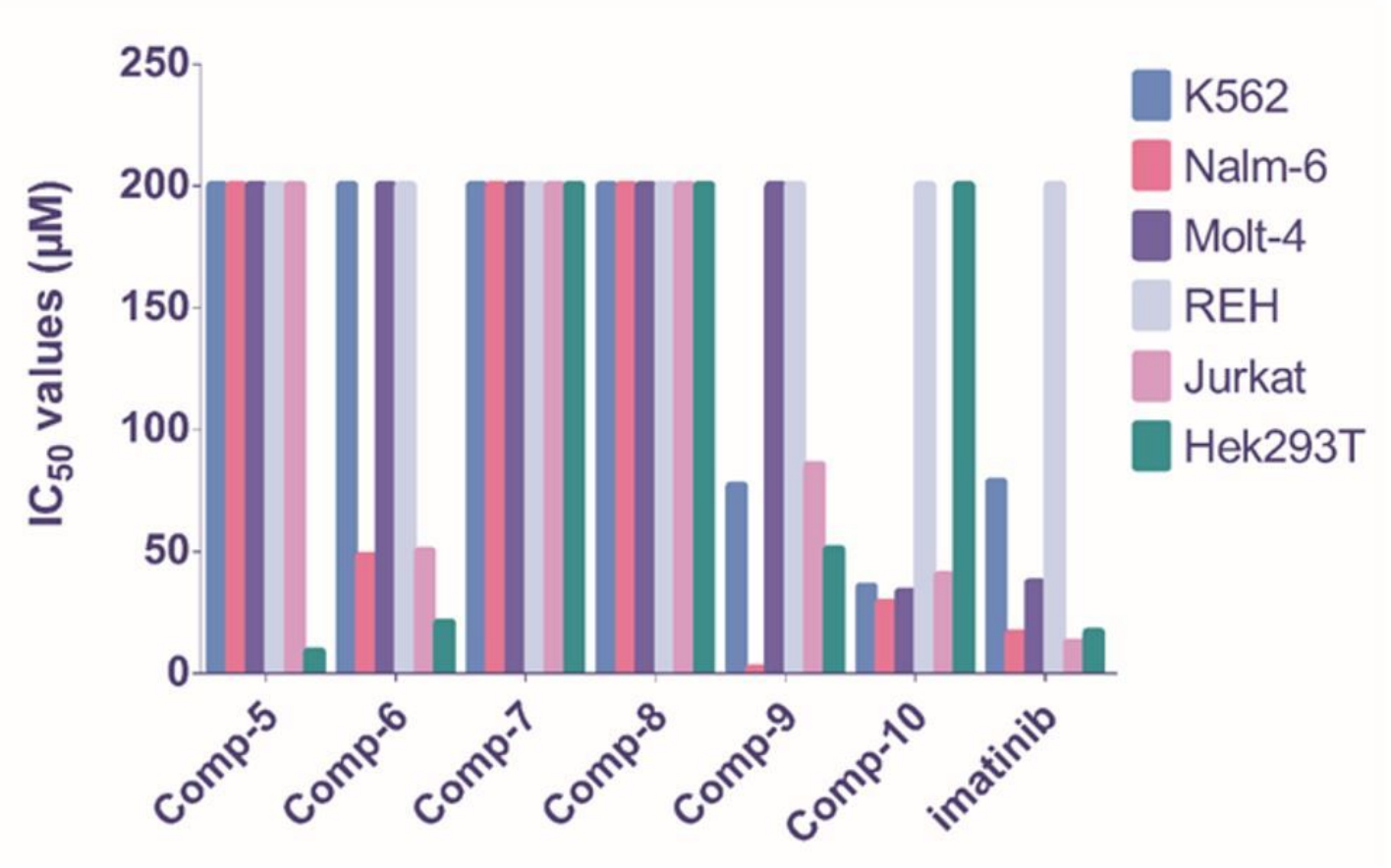

Figure 3

IC50 value of the Compound 5-10 and Imatinib.

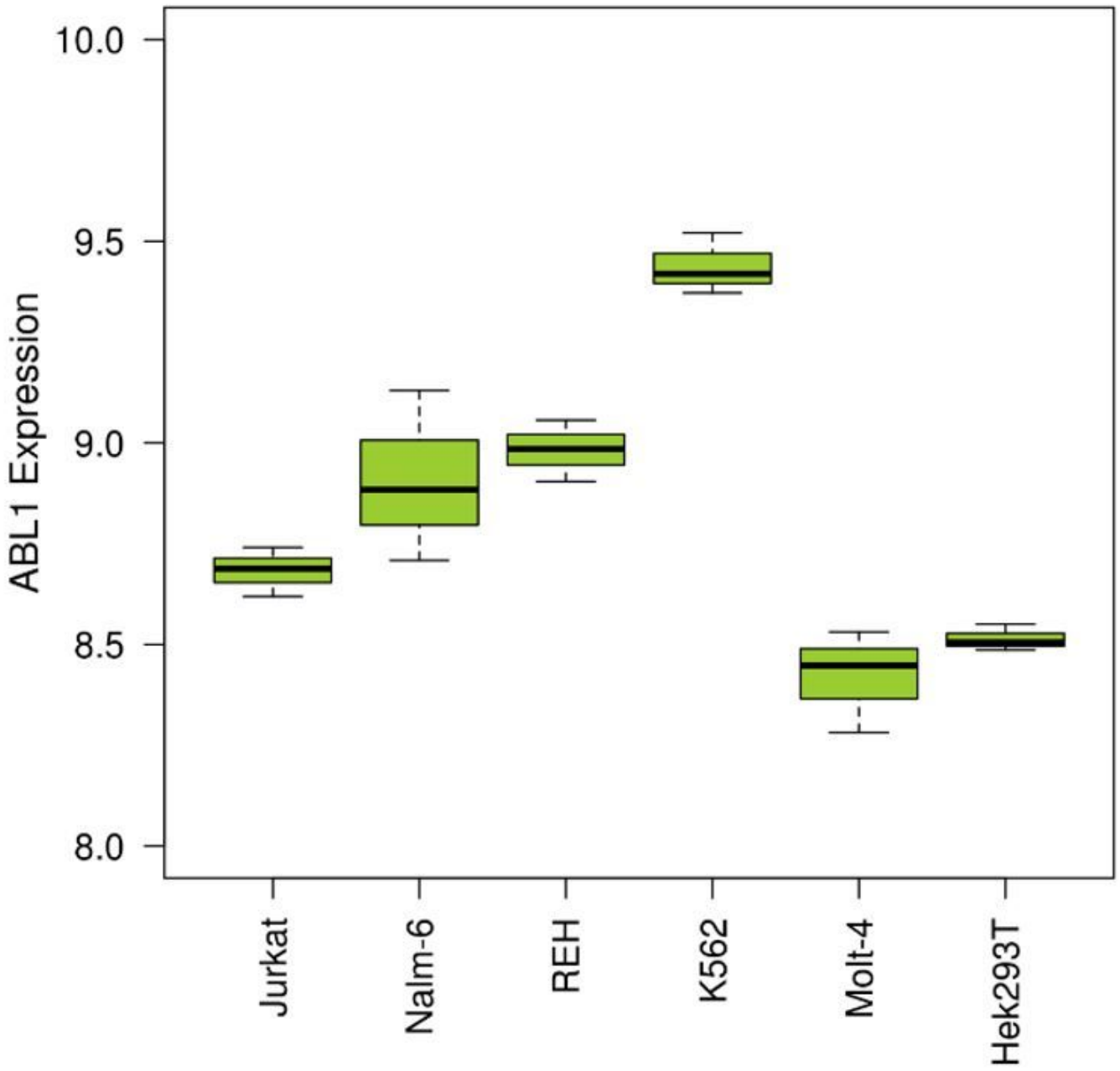

Figure 4

Boxplot of normalized and log2-transformed expression values for Abl1. The figure was generated using graphics package in R version 3.6.3.

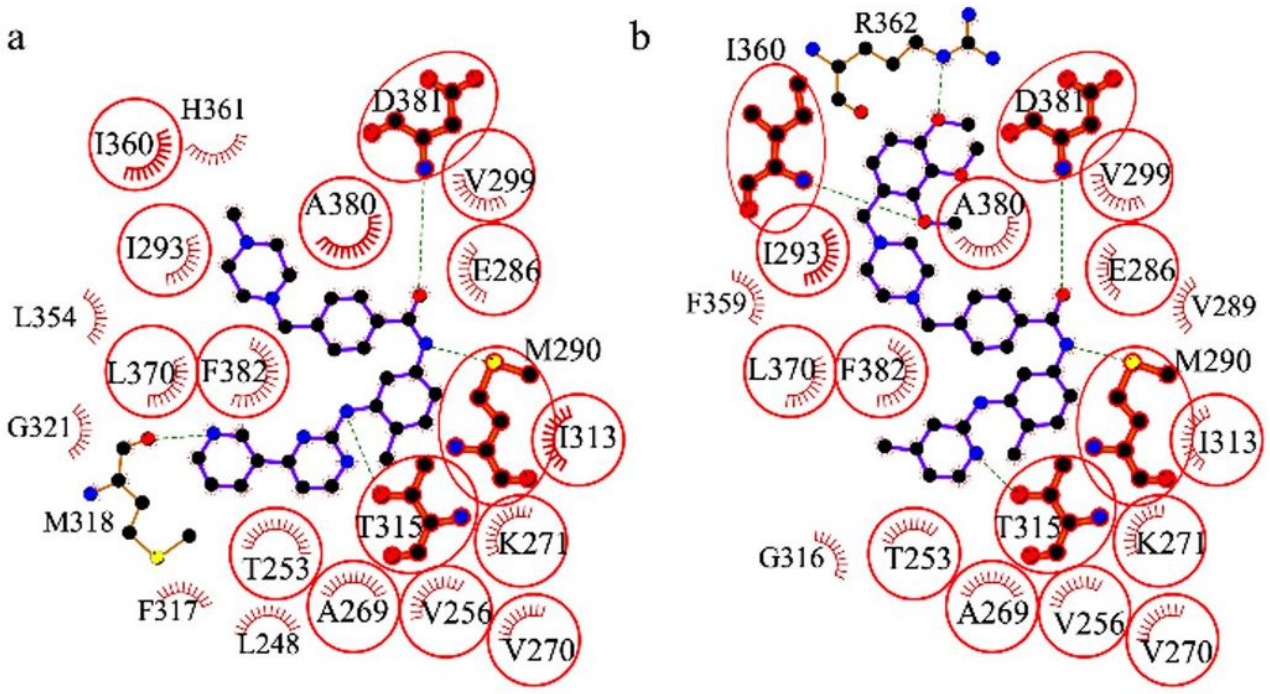

Figure 5

Detailed interactions of ABL1 kinase domain with imatinib (a) and Compound 10 (b). The common contact residues are highlighted with red circles. Hydrogen bonds are indicated by dashed lines, while the hydrophobic interactions are represented by an arc with spokes. The figure was generated using LigPlot+ v.2.2[59].

Supplementary Files

This is a list of supplementary files associated with this preprint. Click to download.

- scheme1.jpg
- graphicsabstract.jpg